

Tracer Dispersion in the Turbulent Convective Layer

ALEX SKVORTSOV, MILAN JAMRISKA, AND TIMOTHY C. DUBOIS

Defence Science and Technology Organisation, Fishermans Bend, Victoria, Australia

(Manuscript received 27 September 2012, in final form 26 June 2013)

ABSTRACT

Experimental results for passive tracer dispersion in the turbulent surface layer under convective conditions are presented. In this case, the dispersion of tracer particles is determined by the interplay of two mechanisms: buoyancy and advection. In the atmospheric surface layer under unstable stratification the buoyancy mechanism dominates when the distance from the ground is greater than the Monin–Obukhov length, resulting in a different exponent in the scaling law for relative separation of Lagrangian particles (a deviation from the celebrated Richardson’s law). This conclusion is supported by atmospheric observations. Exit-time statistics and a probability density function of concentration increments derived from a previously published experimental dataset demonstrate a noticeable difference between tracer dispersion in the convective and neutrally stratified surface layers.

1. Introduction

Understanding transport properties of turbulent convective flow (e.g., transport of particles, chemical species, temperature, etc.) is of significant importance for a number of geoscience fields (meteorology, oceanology, geophysics) covering many practical applications, including pollutant dispersion, extreme events (bushfires, volcanic eruptions, technological catastrophes), cloud formation, and climate change (Franzese et al. 1999; Luhar et al. 2000; Fedorovich 2004; Venkatram 2004; Huang et al. 2009; Sofiev et al. 2009; Klose and Shao 2012; Weil et al. 2012; Jamriska et al. 2012; and references therein). Because of the buoyancy effect and the associated anisotropy, convective turbulence produces a more complex phenomenology than the classical Kolmogorov model of isotropic turbulence, and this imposes new challenges for the development and validation of models of turbulent transport.

Despite of this complexity, there has been remarkable progress in understanding the properties of scalar concentration fields advected by turbulent convective flow, which has emerged from application of the methods of theoretical physics to some simplified systems that

adequately capture phenomenology of real transport processes, with the advantage of being analytically treatable. This theoretical framework, known as scalar turbulence (Shraiman and Siggia 2000), provides rigorous and universal predictions for the statistical properties of scalar concentrations (within the limitations of underlying models) and has received significant attention in recent years. Nowadays, scalar turbulence has become a very broad subject of research that includes analytical and experimental treatments of passive scalar transport, physics-based closures and universal parameterizations for computational fluid dynamics (Biferale et al. 2011; Toschi and Bodenschatz 2008), novel algorithms for data processing (Kunnen et al. 2008; Lohse and Xia 2010; Celani et al. 2004; Bourgoin et al. 2006), and many others. A comprehensive review is outside of the scope of the present study; for more information see Frisch (1996), Falkovich et al. (2001), Sreenivasan and Schumacher (2010), Mazzitelli and Lanotte (2012), and references therein.

Starting with the seminal work of Kraichnan (1968), who calculated statistics of scalar fields dispersed by turbulence with white-noise forcing, the framework of scalar turbulence is now well recognized and appreciated in the field of nonequilibrium statistical physics. This makes it an attractive framework for meteorological applications, since under some conditions (the “passive marker” model), it is reasonable to assume that the fundamental physical properties of turbulent mixing

Corresponding author address: Alex Skvortsov, Defence Science and Technology Organisation, 506 Lorimer Street, Fishermans Bend, VIC 3207, Australia.
E-mail: alex.skvortsov@dsto.defence.gov.au

and not the physical properties or nature of the scalar (e.g., density, chemical composition, size of particles, etc.) determine the statistics of the scalar field. The latter also implies that the statistical predictions of scalar turbulence theory should strongly emerge in experimental observations and computer simulations of atmospheric transport phenomena.

From this perspective, the scalar turbulence framework provides an important tool for universal parameterization and validation of statistical models of convective transport in real geophysical systems. A number of recent publications on this subject (Antonelli et al. 2003, 2005, 2007; Lanotte and Mazzitelli 2013; Mazzitelli and Lanotte 2012) apparently demonstrate the benefits of such an approach to the development of an advanced model of turbulent atmospheric convection. In other publications (Sullivan et al. 1998; Franzese and Borgas 2002; Dosio et al. 2003, 2005; Gioia et al. 2004; Weil et al. 2012) similar assumptions have been successfully employed (i.e., universal scaling of statistical moments of concentrations) without an explicit reference to the scalar turbulence framework.

Despite a vast number of publications on tracer transport in the atmosphere, there is still an evident deficiency in the consistent comparison of real atmospheric observations with the predictions of the scalar turbulence theory (since it has never been a specific objective of these studies). For stable atmospheric conditions, some relevant results can be found in studies by Skvortsov et al. (2010), Yee and Chan (1997), and Jamriska et al. (2012) showing a reasonable agreement with the theory. For convectively dominated transport, alignment with the theory has been less defensible [see some results in Aivalis et al. (2002)], particularly because of the apparent difficulty of data acquisition for convectively dominated transport in the atmosphere [it can occur only during specific times of the day and under specific meteorological conditions (Garratt 1994; Wyngaard 2010)] and the intermittent nature of the convective transport (Sullivan et al. 1998; Fedorovich 2004; Siebesma et al. 2007; Weil et al. 2012). In line with this comment there is a need for extensive and targeted field studies of this phenomenon in order to make more definitive conclusions on the agreement of predictions of the scalar turbulence model with atmospheric observations under convective meteorological conditions. This was the main motivation for the reported study.

In this article we present our experimental results on the statistics of passive tracers in the atmospheric surface layer under convective conditions. The tracer was generated by a very “distributed” source (large-urban-area emissions) providing a continuous (and rather stable) influx of tracer particles in the atmospheric surface

layer. The tracer concentration was measured from a single observation point embedded within the source area. We report statistical properties of the tracer distribution and their alignment with the theoretical conjectures emerging from the scalar turbulence theory.

The outline of the paper is as follows: section 2 presents some results of the scalar turbulence framework relevant to this study, section 3 describes the experimental setup and data acquisition campaign, section 4 discusses experimental results, and some concluding remarks are made in section 5.

2. Framework of scalar turbulence

We restrict our consideration to the case of passive scalars—that is, the scalars whose effect on the flow is negligible (e.g., small aerosol particles). Although we interchangeably refer to the scalar field as tracer particles (appealing to the Lagrangian treatment of scalar turbulence) and scalar concentrations, the framework does not imply a physical existence of such particles [indeed, a tracer can be a gas or temperature (Celani et al. 2004; Lanotte and Mazzitelli 2013; Mazzitelli and Lanotte 2012)]; in other words, the tracer particles can always be viewed as passive markers (or a discrete representation) of the underlying concentration field.

A conventional way to characterize the statistics of scalar fields is to introduce a so-called two-particle correlation function (or structure function of the second order):

$$S_2(r) \equiv \langle [C(\mathbf{x} + \mathbf{r}, t) - C(\mathbf{x}, t)]^2 \rangle \propto r^{\xi_2}, \quad (1)$$

where $C(\mathbf{x}, t)$ is the instantaneous tracer concentration. This formula reflects the assumption that the scalar field is isotropic, homogeneous, and stationary (in the sense of statistical ensemble averaging), so $S_2(r)$ should not depend on the observation point \mathbf{x} nor direction of the separation vector \mathbf{r} . For anisotropic turbulent flows, the structure functions can depend on the direction of \mathbf{r} , but the symmetry of the underlying flow is preserved (Antonelli et al. 2007; Mazzitelli and Lanotte 2012).

The function $S_2(r)$ reveals a deep connection between fluctuations of tracer concentration δC and spatial velocity scaling δv in turbulent flow (Frisch 1997; Falkovich et al. 2001; Celani et al. 2004):

$$S_2(r) \propto (\delta C)^2 \propto r^{\xi_2}, \quad \xi_2 = 2/p, \quad \delta v \propto r^h, \quad p = 2/(1-h). \quad (2)$$

It also establishes the scaling law for the time evolution of the mean interparticle distance R : $dR/dt \propto v$ or

$$R^2 \sim \lambda t^p, \quad (3)$$

where λ is a scale-independent dimensional parameter and the exponent p is dimensionless. The values of parameters λ and p are specific to a particular energy injection mechanism of the turbulent flow; they can often be established based on dimensional grounds (see below). For instance, tracer dispersion by Kolmogorov (locally isotropic) turbulence, $\lambda = \epsilon$ (where ϵ is energy dissipation rate) and $p = 3$ [since $h = 1/3$; Corsin–Obukhov law (Frisch 1997; Falkovich et al. 2001; Celani et al. 2004)], and buoyancy dominated turbulence, $p = 5$ [$h = 3/5$; Bolgiano–Obukhov law (Celani et al. 2004)]. For a turbulent flow with a linear velocity profile (constant shear), it was deduced that $p = 6$ (for particle separation along the mean velocity) and $p = 4$ (for separation in the transverse direction), with λ being a function of the velocity gradient (Celani et al. 2005).

In the turbulent surface layer where boundary effects dominate at the large- t limit, the parameter p may attain different values (Skvortsov et al. 2010; Yee and Skvortsov 2011). Since the tracer particles are “trapped” in the mixing layer, at some point R reaches the scale of the mixing layer, and the tracer dispersion effectively becomes two dimensional. The vertical scale of this capping (i.e., transition to two-dimensional dispersion) can be associated with vertical changes of the meteorological parameters (i.e., scales of layered structure in the atmospheric boundary layer) that depend on specific meteorological conditions; see Garratt (1994) and Wyngaard (2010). For the convective boundary layer it can be described in terms of boundary layer thickness z_i , the surface-based inversion depth or thickness of the surface layer z_s , and the Monin–Obukhov length L_{mo} . The appropriate estimates for p for two-dimensional dispersion can be heuristically derived based on a straightforward dimensional analysis and the fact that in the turbulent surface layer under neutral conditions the friction velocity v_* (and not a dissipation rate ϵ) is a dimensional parameter controlling the turbulent motion. Therefore, in (3), $R^2 \sim (v_* t)^2$, which implies that $p = 2$ and $\lambda = v_*^2$ [the “ballistic” regime (Skvortsov et al. 2010)]. Similar reasoning can be applied to the convective boundary layer leading to $\lambda = w_*^2$ and $p = 2$, where w_* is the scale convective velocity (see below). It is noteworthy that the ballistic asymptotes correspond to the lowest value of p .

From the above comments it can be concluded that different values of parameter p (or scaling exponent ξ_2) can be used as a signature of a particular mechanism of tracer dispersion. This was the main theoretical assumption for the present study, which we validate against experimental data.

For single-point concentration measurements (as in our experimental setup), analysis of the time series of tracer concentrations is limited to data obtained from a single location. In these cases, the Taylor frozen-turbulence hypothesis is invoked in order to link measurements in time with measurements in space (Monin and Yaglom 1975a,b). In other words, the concentration increment at the separation distance r is obtained by measuring the concentration over a time difference $\delta t = \delta r/U$, where U is the mean velocity of the flow (wind). Therefore, (2) leads to

$$S_2(r) \propto (\delta C)^2 \propto (Ut)^{2p}. \quad (4)$$

There is no general justification for an application of the frozen-turbulence hypothesis to the analysis of any experimental dataset of tracer dispersion (Monin and Yaglom 1975a,b); however, some supporting arguments can be made based on relatively low fluctuations of flow velocity during the time of our observations. The latter conditions were typical for the datasets presented and gave us an opportunity to evaluate the accuracy of the frozen-turbulence hypothesis within this framework (Wyngaard and Clifford 1977 and references therein).

A great variety of methods have been proposed to analyze time series of tracer concentration advected by turbulent flow and to infer parameters of the underlying tracer statistics. The method of exit-time statistics (Biferale et al. 2001; Celani et al. 2004) has proved to be a robust tool to recover nontrivial scaling properties of tracer distributions and relate them to the fundamental physics of turbulent mixing. This method was employed in this study to validate theoretical conjectures for parameter p discussed above.

Exit-time statistics are based on detection of time intervals where a measured value of concentration exits through a set of thresholds δC (Biferale et al. 2001; Celani et al. 2004). By scanning the time series for a given threshold, one can recover a set of times $\tau_i(\delta C)$ for which the measured concentration crosses this threshold. This set can then be used to calculate the inverse structure function [for details, see Celani et al. (2004)]:

$$\Sigma_q(\delta C) \equiv \langle \tau^q(\delta C) \rangle, \quad (5)$$

where q is an index of statistical moment of τ .

A comprehensive analysis of the properties of the inverse structure function can be fulfilled by applying the well-known multifractal approach (Biferale et al. 2001; Boffetta et al. 2008; Schmitt 2005). This results in the following scaling:

$$\Sigma_q(\delta C) \propto (\delta C)^{\chi(q)}, \quad (6)$$

where exponent $\chi(q)$ is believed to be a linear function of q (with no intermittency correction). The function $\chi(q)$ may have different asymptotes for $q < 1$ and $q > 1$ caused by the effect of large-scale (smooth) turbulent fluctuations. Another constraint follows from (2) and (4):

$$\chi(1) = p, \quad (7)$$

and reflects the fact that $\Sigma_q(\delta C)$ should comply with the dimensional analysis [which amounts to the scaling law $\tau \propto (\delta C)^p$].

It is worth noting that $\Sigma_q(\delta C)$ is formally defined for any $q > 0$ (and not only for natural numbers). We calculated the function $\chi(q)$ using our experimental dataset.

Now we briefly comment on how the above theoretical conjectures (based on rather restrictive assumptions) can be applied to real atmospheric observations. We assume that a single observation point is located at some height H above the ground. We begin with a simple case, when the effect of thermal flux is insignificant (neutral stratification; Garratt 1994; Wyngaard 2010). For $R \ll H$ (or expressed in time domain as $t \ll H/v_*$) the turbulence may be considered as quasi isotropic, so we may expect initially $p \approx 3$. For particles released near the ground the effect of the boundary will eventually dominate (at $R \gg H$), so it is reasonable to expect that p will approach the ballistic asymptote $p = 2$. Convergence to ballistic may be nonmonotonic, since at intermediate times $t \sim H/v_*$ the tracer dispersion may be dominated by the shear effect, leading to higher values of p ($4 \leq p \leq 6$). The likelihood of this “shear” increase strongly depends on the local wind profile (it exists only in quasi-linear velocity profiles).

For the case when heat flux dominates (turbulent convective flow) the situation is more complex. This complexity is due to the intermittent character of the flow (and tracer transport) in the convective boundary layer caused by evolution of large-scale thermal plumes. These create an ever-changing distribution of vertical flows (updrafts/downdrafts) and associated tracer structures with a strong spatial and temporal inhomogeneity (Sullivan et al. 1998; Siebesma et al. 2007; Weil et al. 2012; Lanotte and Mazzitelli 2013). The analytical description of this complexity leads to an appearance of the new scales for velocity: Deardorff’s convective velocity scale w_* and length L_{mo} . These scales are defined as $w_* = (z_i Q g / T)$ and $L_{mo} = -(v_* / w_*)^3 (z_i / \kappa)$, where z_i is the depth of the convective layer; g gravitational acceleration; Q and T are heat flux and temperature at the ground, respectively; and $\kappa = 0.4$ (Garratt 1994; Wyngaard 2010). The mixing layer, $L_{mo} < z < z_i$, is characterized by an intensive mixing, so tracers in this

layer are believed to be in a well-mixed state (except for a narrow region near the inversion layer at the top) and exhibit a rather universal statistical distribution (Sullivan et al. 1998; Fedorovich 2004; Weil et al. 2012; Lanotte and Mazzitelli 2013; Mazzitelli and Lanotte 2012). One can assume that a signature of the convectively dominated regime of tracer transport (i.e., $p = 5$) should clearly emerge if one manages to obtain measurements of tracer statistics from above the surface layer (i.e., inside the mixing layer). This assertion can be translated to two apparent conditions: $H > |L_{mo}|$ and $w_* \gg v_*$. These conditions were used as criteria in selecting appropriate datasets from our observation campaign. Some revealing numerical examples to support this reasoning are presented in Calzavarini et al. (2002), Lanotte and Mazzitelli (2013), and Mazzitelli and Lanotte (2012).

This phenomenological reasoning allows us to draw the following conclusions regarding temporal evolution of the parameter p in the convective boundary layer. Initially, one expects $p \approx 3$, which, on small scales of turbulence, can still be considered as quasi isotropic ($t \ll H/w_* \ll H/v_*$). Then p should approach the “convective” value $p = 5$ and finally at the large time limit it should decay to the ballistic asymptote $p = 2$ (Skvortsov et al. 2010).

The theoretical conjectures discussed above, being deduced from rather idealized models, may be overshadowed by profound effects typically associated with the dynamics of real meteorological flows (strong spatial inhomogeneity, nonstationarity of thermal flux, entrainment events, etc.). Even a simple order-of-magnitude estimation of the contribution of such effects would require sophisticated computer simulations (Sullivan et al. 1998; Fedorovich 2004; Weil et al. 2012; Lanotte and Mazzitelli 2013) and is far outside of the scope of our study. Nevertheless, we anticipate that the predicted values of p should emerge from our experimental data, dictated by the universal mechanisms of turbulent mixing.

3. Experimental procedure

The presented data were collected during a monitoring campaign aimed at the physical characterization of ambient air background content for an urban/industrial type of outdoor environment. Only a brief outline of the campaign is presented here, as detailed information about the experimental instrumentation, sampling methods, measurement site, and data analysis can be found elsewhere (Jamriska et al. 2012).

The measurements were conducted in Port Melbourne located close to Melbourne’s central business district (CBD). In total, 500 h of data (5-s readings) were recorded from a measurement campaign spanning 28 days

during April–July 2009 using a suite of aerosol instruments (Jamriska et al. 2012). The monitoring was done on a semicontinuous basis with interruptions in sampling due to instrument maintenance and availability. Data used in this study were measured by an optical spectrometer (Dycor 2013). The measured parameters included concentration and size distribution of aerosol particles in the 1–10- μm size range. Particles of this size can be considered as passive scalars, since their size and negligible volume fraction have little effect on the airflow field (Ottino 1989; Aref 1995). Air sampling was done on a top of a four-story building at a height of 12 m. The measuring equipment was located in an air-conditioned enclosure with sampling points protruding approximately 1.5 m outside of the enclosure's roof.

Anthropogenic activity [for details, see Jamriska et al. (2012)] in the surrounding urban area (roughly 20 km in size) provided a continuous (and relatively stable) influx of aerosol particles into the measured atmospheric flow. Analysis of the data (scaling relationships between statistical moments of tracer concentration) revealed the ambient air can be considered well mixed [as was verified in Jamriska et al. (2012) with a consistent intermittency value of 0.97].

The collected data were screened for outliers, evaluated, processed, and then imported into an in-house-developed database. A set of software tools was also developed, allowing manipulation and retrieval of user-defined data/subsets for further analysis. Particle concentration fluctuated during the day, showing a diurnal character. The variation could be associated with changes in traffic volume during the day and increased effects of anthropogenic sources observed during the night. Further analysis of aerosol concentration and size characteristics for all collected data (i.e., measured for all atmospheric conditions), exploratory statistics, and time series analysis are presented elsewhere (Jamriska et al. 2012; Skvortsov et al. 2010). Comparison of the measured results with literature data for the Melbourne area showed very good agreement (Jamriska et al. 2012 and references therein).

Surface-bounded turbulent flow under the effect of changing stratification provides flexible settings to study the relative contribution of the buoyant and kinetic energy fluxes on scalar transport—since this contribution can be easily controlled by varying the distance to the underlying surface (and passing the threshold of the Monin–Obukhov length) (Calzavarini et al. 2002; Bistagnino et al. 2007; Boffetta et al. 2008). To validate this assumption, meteorological data (hourly averages for surface data, vertical profile data recorded every 5–6 h) were obtained from a local meteorological station operated by the Bureau of Meteorology (BOM) as well

as from local measurements at the sampling site with 1-min averaging (Vaisala MAWS201M instrument). Data from both sites were compared and showed good correlation.

BOM data were used to characterize atmospheric conditions of the surface layer (stability, vertical and horizontal profiles of wind speed, temperature, and pressure) and to calculate w_* , v_* , and L_{mo} . These parameters were determined using the profile method as outlined in Van Ulden and Holtslag (1985).

Overall, two subsets of continuous data (of 10 h in duration) were identified and presented in this study to support the theoretical conjectures discussed above. These subsets were selected based on a number of meteorological criteria: ambient air temperature needed to be high enough to allow development of convective flow (more specifically, $w_* > v_*$), mean wind speed U_H needed to be rather low to negate any wind shear dominance (to mitigate commutative increase of p during intermediate time of observations), and the height of sampling tower should exceed the Monin–Obukhov length ($H > |L_{\text{mo}}|$) to verify the tracer particles were indeed in the convective regime. Operational constraints of our experiment imposed additional challenges for selection of good quality datasets: confining selection to times when the monitoring system operated without disruption and associated meteorological data were available.

4. Results

Initial correlation analysis of the concentration time series $C(t)$ of single-point measurements shows that the minimum time span required to obtain reliable statistics of the process should be more than 3 h (Skvortsov et al. 2010). Following this analysis we employed Taylor's hypothesis to calculate $S_2(r)$ from (4). Parameter p was estimated [by plotting $S_2(r)$ on a log–log scale] and compared with the theoretical predictions. Some examples of these plots are depicted in Fig. 1.

The application of Taylor's hypothesis for the estimation of tracer statistics in turbulent convective flows has recently been the focus of a number of studies [for details, see He et al. (2010), Zhou et al. (2011), and Higgins et al. (2012)]. The level of velocity fluctuations in this case is relatively high, and conditions of the traditional Taylor frozen-turbulence hypothesis may be violated (Monin and Yaglom 1975a,b; He et al. 2010; Zhou et al. 2011). To overcome this difficulty, a simple but universal modification to Taylor's framework has been proposed in He et al. (2010) and Zhou et al. (2011), where the frozen-turbulence hypothesis can still be applied for single-point concentration measurements—provided one substitutes a “redefined” convective velocity

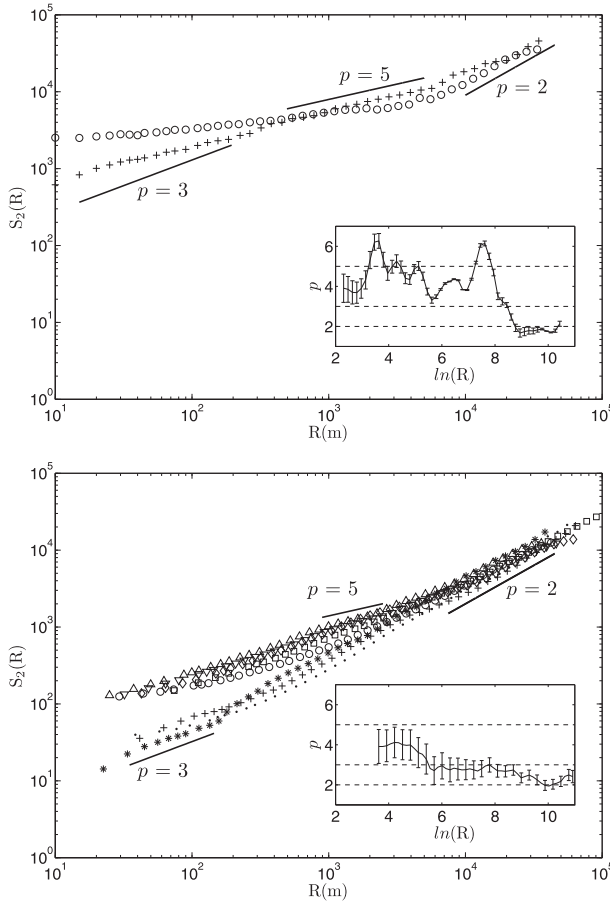


FIG. 1. Structure functions of the tracer concentration $S_2(R) \propto R^{2p} \propto (U_H t)^{2p}$ on log–log scales: (top) convective conditions and (bottom) neutral conditions (Skvortsov et al. 2010). Insets show the evolution of the scaling parameter p of the mean interparticle displacement and error bars correspond to plus or minus the mean standard deviation. Each dataset in the convective conditions plot corresponds to 10 h of observations; meteorological conditions for these periods are outlined in Table 1: sample 1 (plus signs) and sample 2 (circles); $p \approx 3$ is the Richardson (Corsin–Obukhov) regime, $p \approx 5$ is the convective (Bolgiano–Obukhov) regime, and $p \approx 2$ is the ballistic regime.

using the linear relationship $\delta t = \delta_r/U_c$ or, more specifically, $U_c = (U_H^2 + \sigma_U^2)/U_H$, where σ_U is the standard deviation of the wind velocity (see Table 1). This redefined framework has been used throughout our study.

As stated previously, the main aim of the present study was to perform data analysis to recover statistics of tracer distributions in the turbulent surface layer under strong convective conditions; however, some

results observed for neutral conditions that have been reported previously (Skvortsov et al. 2010) are also presented for comparison.

As elaborated above, for the short time limit the scalar statistics can be described by the Kolmogorov–Corsin–Obukhov law and hence we expect to recover the classical Richardson regime with $p = 3$ for both convective and nonconvective regimes. At asymptotically long times (theoretically infinite) we may also expect that p approaches its global ballistic asymptote (viz. $p = 2$ for both cases). In the convection dominated regime, the $p = 5$ maximum should always emerge; while for neutral conditions a similar maximum ($4 \leq p \leq 6$) may occasionally occur (since it is very specific to the local velocity profile).

In general, our experimental results support these theoretical predictions (see insets in Fig. 1). The occasional maxima of $p \approx 5$ is visible in some datasets corresponding to nonconvective conditions and are always present in convectively dominated cases, monotonically approaching the convective value $p = 5$. Finally, at longer times the ballistic asymptote also appears in the convectively dominated regime.

It is worth noting that the long-time ballistic limit $p = 2$ for the nonconvective regime is in agreement with the recent experimental data on atmospheric dispersion $2 \leq p \leq 3$ (Mikkelsen et al. 2002, Salazar and Collins 2009, and references therein).

To illustrate the meteorological context for our study, vertical profiles of virtual temperature and wind velocity are presented in Fig. 2. Some meteorological parameters (w_* , v_* , U_H , L_{mo} , z_s , and z_i) are also listed in Table 1. These parameters were either measured directly (U_H and temperature) or calculated from local meteorological data (BOM) for each observation period [see Van Ulden and Holtslag (1985) for details].

The meteorological profiles are depicted in Fig. 2. They exhibit profound surface-based inversion layers at rather low altitudes ($z_s \approx 87$ and 52 m). It is known that meteorological flows corresponding to such conditions are characterized by a rich variety of lengths and time scales (McNaughton et al. 2007) as well as significant complexity in the dynamics of the atmospheric mixing layer (intermittency of entrainment flux, spatial variations, strong updrafts/downdrafts near the top of the surface layer) (Sullivan et al. 1998; Siebesma et al. 2007; Weil et al. 2012; Lanotte and Mazzitelli 2013). This

TABLE 1. Meteorological conditions prevalent during buoyancy-dominated turbulence as shown by samples displayed in Fig. 1.

Sample	U_H (m s ⁻¹)	L_{mo} (m)	v_* (m s ⁻¹)	w_* (m s ⁻¹)	z_s (m)	z_i (m)
1 (plus signs)	2.75 ± 0.40	−1.66	0.05	0.52	87.5	727.5
2 (circles)	2.26 ± 0.53	−1.70	0.04	0.45	52.5	1390.5

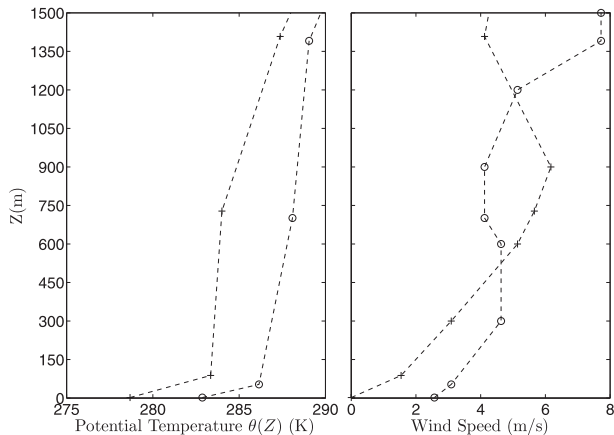


FIG. 2. Vertical profiles of (left) potential temperature and (right) wind speed corresponding to the meteorological conditions recorded at the times of sample 1 (plus signs) and sample 2 (circles) from Fig. 1.

complexity may significantly influence the tracer transport in the surface layer, although our results show that a physics-based scaling approach can still be used to describe convective transport under these complex meteorological conditions.

We remark here that the vertical meteorological profiles of wind velocity and temperature were taken once per dataset (twice at best) without any reference to the beginning of the sampling period and they should be used only as indicative values. Any dynamic observations of the evolution of these profiles were not available and any predictions of such an evolution (say evolution of z_i , z_s , and L_{mo} scales) is rather speculative. For instance, some anomalies of data presented in Fig. 1 (early onset of the convective scaling) can be explained by a possible violation of the condition $H < z_s$ (since the convective boundary layer was developing during the sampling period). Another possible explanation of these anomalies can be related to an intensive thermal plume that formed in proximity of the observation point (Sullivan et al. 1998; Siebesma et al. 2007; Weil et al. 2012; Lanotte and Mazzitelli 2013); such a plume could provide a strong localized flux of particles from the mixing layer that penetrates into the surface layer. Although both of these explanations are definitely plausible, without meteorological data of high resolution (spatial and temporal), it is difficult to support and validate any such far-reaching conclusions.

To reveal further differences between particle transport in convective and neutrally stratified turbulent surface layers, we employ the algorithm of exit-time statistics for the concentration time series and compute the inverse structure function using (6), which estimates the scaling exponent $\chi(q)$.

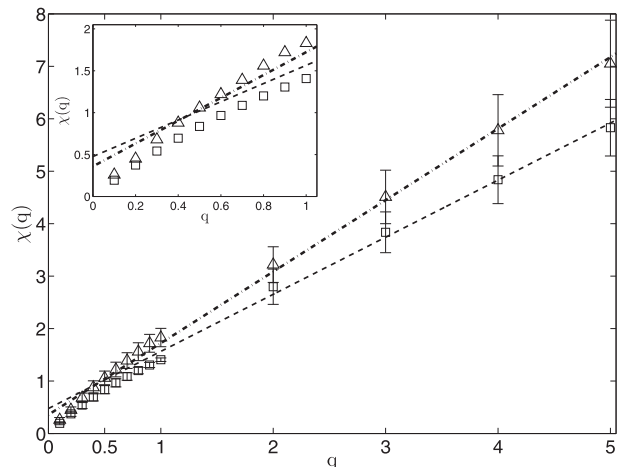


FIG. 3. Mean inverse structure function for experimental datasets displayed in Fig. 1: convective conditions (squares) and neutral conditions (triangles) (Skvortsov et al. 2010). Error bars correspond to plus or minus the mean standard deviation. The thin dashed (convective) and thick dashed-dotted (neutral) lines represent a linear best fit over $1 \leq q \leq 5$ predicted by (6) (Schmitt 2005). Inset shows the nonlinear trend where $q < 1$, which is attributed to differentiable components of the atmospheric turbulence.

Similar to particle dispersion in nonconvective conditions, analysis of the results for the convective regime leads to the conclusion that $\chi(q)$ is a linear function of q (Schmitt 2005). We observe that $\chi(q)$ seems to follow the predicted linear trend for $q \geq 1$, but with a noticeably smaller gradient than in the neutral surface layer case (1.1 and 1.3 for convective and neutral conditions, respectively). The reference values are $\chi(1) = 1.4$ (convective regime) and $\chi(1) = 1.8$ (neutral stratification), which is in reasonable agreement with the theoretical prediction in (7).

As explained in Celani et al. (2004) and Boffetta et al. (2008), a nonlinear response near the threshold value $q = 1$ (if it exists) can be attributed to a contribution from slow (differentiable) components of turbulent motion. In our observations we found that this change is usually less profound for the turbulent convective surface layer (see Fig. 3).

The scaling laws for concentration statistics discussed above provide insight into important statistical characteristics of the concentration time series in the form of the probability density function (PDF) of tracer fluctuations (or concentration increments) (Antonelli et al. 2003, 2005, 2007; Lanotte and Mazzitelli 2013; Mazzitelli and Lanotte 2012), which is presented in Fig. 4.

According to scaling arguments discussed above, the PDF of concentration increments can be written in a self-similar form (see also Antonelli et al. 2003, 2005, 2007; Lanotte and Mazzitelli 2013; Mazzitelli and Lanotte 2012):

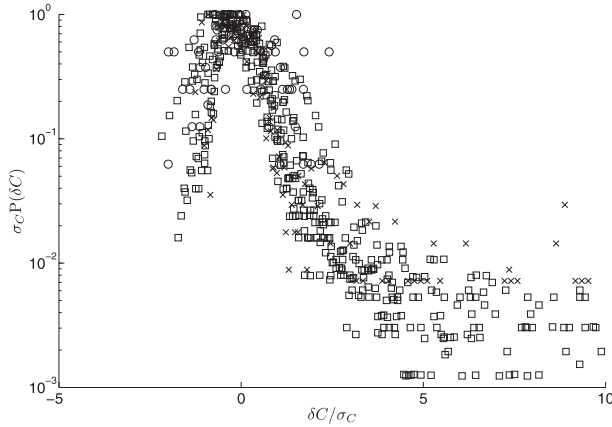


FIG. 4. PDF of concentration increments, based on (8). Markers correspond to data points from different regimes of tracer dispersion: Richardson (circles), convective (crosses), and ballistic (squares) regimes.

$$P(\delta C) = \frac{1}{\sigma_C} \Phi(\zeta), \quad \zeta = \delta C / \sigma_C, \quad (8)$$

where $\Phi(\zeta)$ is an unknown (but universal) function, $\delta C = C - \langle C \rangle$, and $\sigma_C^2 = \langle C^2 \rangle - \langle C \rangle^2$. The time dependency of σ_C^2 follows from the estimate $\sigma_C^2 \propto S_2(t)$ and the scaling law [(2)]; hence, $\sigma_C \propto t^\alpha$, where exponent α is, generally speaking, a function of time with limiting values $\alpha = \{1/3, 1/5, 1/2\}$ corresponding to the Richardson, convective, and ballistic regimes, respectively.

The PDF defined by (8) gives the likelihood (probability) of observing a fluctuation δC during a time interval t . To evaluate function $\Phi(\zeta)$ and to validate the scaling law $\sigma_C \propto t^\alpha$, we implemented the following algorithm. The entire dataset was cut into a large number of slices (time intervals), and each interval had a random span and a random initial point. For each time interval the function $P(\delta C)$ was estimated from the histogram of concentration fluctuations occurring during that interval, and parameter α was prescribed from the set $\{1/3, 1/5, 1/2\}$ depending on the length of the interval (whether the time interval falls into the Richardson, convective, or ballistic regime). The final results were plotted as function $t^\alpha P(\delta C) = \Phi(\zeta)$ against $\zeta = \delta C / t^\alpha$. The collapse of all histograms for concentration increments (i.e., estimations from different time intervals) to a single profile supports our conjecture for the scaling law $\sigma_C \propto t^{\alpha(t)}$ as well as the existence of a universal PDF for concentration increments [i.e. a universal function $\Phi(\zeta)$]. A functional fit for $\Phi(\zeta)$ will be presented in a separate publication. For a review of possible functional forms of concentration fluctuations in the convective boundary layer see Sykes (1988), Weil et al. (1992), and Dosio and Vilá-Guerau de Arellano (2006).

It is noteworthy that the shape of this PDF is quantitatively similar to one presented in other studies

(Antonelli et al. 2003, 2005, 2007; Lanotte and Mazzitelli 2013; Mazzitelli and Lanotte 2012).

5. Concluding remarks

We presented experimental results for passive tracer dispersion in the turbulent convective layer when the dispersion of particles was dominated by buoyancy fluxes. We found that our observations can be intrinsically explained with a three-stage model of tracer dispersion. During the first stage of separation, turbulence can be considered as quasi isotropic and tracer particles obey the standard Richardson model. During the next stage, particle separation follows the “fast” regime of convective dispersion (predicted by Bolgiano–Obukhov scaling). During the last stage (the long time limit) particle motion is bound to the two-dimensional substructure (mixing layer), and we observed the ballistic regime of particle separation. The scatter of the data is more significant than that for dispersion in neutral conditions and this is in line with other publications that reported intermittent tracer flux in the convective boundary layer (usually attributed to the motion of thermal plumes in the convective layer). The presented results may have implications for the study of convective phenomena in various meteorological conditions and may assist in reducing the appreciable uncertainty in the prediction of tracer distributions.

Some statistical parameters estimated in our study may have significance for practical applications and this deserves a brief comment. Understanding scaling properties of the second-order structure function [(4); i.e., the scaling law of concentration fluctuations] is an important step in development of high-fidelity models of pollutant transport, since it is vital for the correct estimation of many operational parameters (pollutant exceedance probabilities, integrated toxic load, peak-to-mean ratio, etc.). It also provides a rigorous framework for the development of simplified models (or surrogate simulation) of tracer statistics from deterministic models of pollutant dispersion (i.e., for generation of synthetic time series of tracer concentration) and that would significantly increase the fidelity and predictive skills of these models (Bisignanesi and Borgas 2007; Gunatilaka et al. 2012). More specifically, one can employ a PDF of tracer concentration in the form of (8), where $\langle C \rangle$ is the ensemble mean at a given location (given by a deterministic model), p is defined in (2), and U is wind velocity; see (4). Such simplified models may become important for the rapid evaluation of numerous “what if” scenarios, especially in cases when such evaluation is impossible (or computationally demanding) to perform using other methods (i.e., hazardous risk assessment,

operational planning for first responders, etc.) (Gunatilaka et al. 2012). The functional form of the PDF $\Phi(\xi)$ can be further refined by its comparison with experimental studies (Bisignanesi and Borgas 2007; Borgas et al. 2013, manuscript submitted to *Bound.-Layer Meteor.*) or by calibration with the results of more advanced models (i.e., Lagrangian particles, large-eddy simulations) (Sullivan et al. 1998; Fedorovich 2004; Weil et al. 2012; Lanotte and Mazzitelli 2013).

In line with the above comment, exit-time statistics and the concentration increments PDF in (8) are critical for the design of environmental monitoring systems. In fact, the scaling law $\tau^g \propto (\delta C)^{\chi(g)}$ [or its simplified form $\delta C \propto \tau^{\alpha(\tau)}$] describes the statistics of a typical time to observe a fluctuation δC . Inversely, it describes the likelihood of an expected tracer fluctuation δC during a given time span τ . In the context of monitoring system design, they provide a rigorous functional relationship between such important parameters as time to detect (for a given concentration exceedance) and expected detection threshold (for a given time of observation), as well as the probability of false alarms, and enables a consistent evaluation of system prototypes (Mendis et al. 2012). Another interesting application of the proposed framework is to develop a data fusion algorithm for the continuous estimation of parameter α from the concentration time series in order to infer the stability conditions of atmospheric surface layer.

We anticipate that the results presented in this study can be useful in evaluating dispersion models for tracer transport and systems for environmental monitoring.

Acknowledgments. We thank the three anonymous referees for their valuable comments to the manuscript and their constructive suggestions. We are grateful to Alex Hill for assistance with obtaining meteorological data.

REFERENCES

- Aivalis, K. G., K. R. Sreenivasan, Y. Tsuji, J. C. Klewicki, and C. A. Biloft, 2002: Temperature structure functions for air flow over moderately heated ground. *Phys. Fluids*, **14**, 2439–2446, doi:10.1063/1.1485079.
- Antonelli, M., A. Mazzino, and U. Rizza, 2003: Statistics of temperature fluctuations in a buoyancy-dominated boundary layer flow simulated by a large eddy simulation model. *J. Atmos. Sci.*, **60**, 215–224.
- , M. M. Afonso, A. Mazzino, and U. Rizza, 2005: Structure of temperature fluctuations in turbulent convective boundary layers. *J. Turbul.*, **6** (35), 35–69.
- , A. Lanotte, and A. Mazzino, 2007: Anisotropies and universality of buoyancy-dominated turbulent fluctuations: A large-eddy simulation study. *J. Atmos. Sci.*, **64**, 2642–2656.
- Aref, H., 1995: *Chaos Applied to Fluid Mixing*. Pergamon Press, 370 pp.
- Biferale, L., M. Cencini, A. Lanotte, D. Vergni, and A. Vulpiani, 2001: Inverse statistics of smooth signals: The case of two dimensional turbulence. *Phys. Rev. Lett.*, **87**, 124501, doi:10.1103/PhysRevLett.87.124501.
- , F. Mantovani, M. Sbragaglia, A. Scagliarini, F. Toschi, and R. Tripiccione, 2011: Second order closure for stratified convection: Bulk region and overshooting. *J. Phys.: Conf. Ser.*, **318**, 042018, doi:10.1088/1742-6596/318/4/042018.
- Bisignanesi, V., and M. Borgas, 2007: Models for integrated pest management with chemicals in atmospheric surface layers. *Ecol. Modell.*, **201**, 2–10, doi:10.1016/j.ecolmodel.2006.07.040.
- Bistagnino, A., G. Boffetta, and A. Mazzino, 2007: Lagrangian velocity structure functions in Bolgiano turbulence. *Phys. Fluids*, **19**, 011703, doi:10.1063/1.2432154.
- Boffetta, G., A. Mazzino, and A. Vulpiani, 2008: Twenty-five years of multifractals in fully developed turbulence: A tribute to Giovanni Paladin. *J. Phys.*, **41A**, 363001, doi:10.1088/1751-8113/41/36/363001.
- Bourgoin, M., N. T. Ouellette, H. Xu, J. Berg, and E. Bodenschatz, 2006: The role of pair dispersion in turbulent flow. *Science*, **311**, 835–838, doi:10.1126/science.1121726.
- Calzavarini, E., F. Toschi, and R. Tripiccione, 2002: Evidences of Bolgiano-Obukhov scaling in three-dimensional Rayleigh-Bénard convection. *Phys. Rev.*, **66E**, 016304, doi:10.1103/PhysRevE.66.016304.
- Celani, A., M. Cencini, A. Mazzino, and M. Vergassola, 2004: Active and passive fields face to face. *New J. Phys.*, **6**, 72, doi:10.1088/1367-2630/6/1/072.
- , —, M. Vergassola, E. Villermaux, and D. Vincenzi, 2005: Shear effects on passive scalar spectra. *J. Fluid Mech.*, **523**, 99–108, doi:10.1017/S0022112004002332.
- Dosio, A., and J. Vilà-Guerau de Arellano, 2006: Statistics of absolute and relative dispersion in the atmospheric convective boundary layer: A large-eddy simulation study. *J. Atmos. Sci.*, **63**, 1253–1272.
- , —, A. A. M. Holtslag, and P. J. H. Builtjes, 2003: Dispersion of a passive tracer in buoyancy- and shear-driven boundary layers. *J. Appl. Meteor.*, **42**, 1116–1130.
- , J. V.-G. de Arellano, and A. A. M. Holtslag, 2005: Relating Eulerian and Lagrangian statistics for the turbulent dispersion in the atmospheric convective boundary layer. *J. Atmos. Sci.*, **62**, 1175–1191.
- Dycor, 2013: CFLAPS: Fluorescent Aerosol Particle System. [Available online at <http://www.dycor.com/Products/DefenseSecurity/CBRNESurveillanceSolutions/CFLAPS.aspx>.]
- Falkovich, G., K. Gawedzki, and M. Vergassola, 2001: Particles and fields in fluid turbulence. *Rev. Mod. Phys.*, **73**, 913–975, doi:10.1103/RevModPhys.73.913.
- Fedorovich, E., 2004: Dispersion of passive tracer in the atmospheric convective boundary layer with wind shears: A review of laboratory and numerical model studies. *Meteor. Atmos. Phys.*, **87**, 3–21, doi:10.1007/s00703-003-0058-3.
- Franzese, P., and M. S. Borgas, 2002: A simple relative dispersion model for concentration fluctuations in contaminant clouds. *J. Appl. Meteor.*, **41**, 1101–1111.
- , A. K. Luhar, and M. S. Borgas, 1999: An efficient Lagrangian stochastic model of vertical dispersion in the convective boundary layer. *Atmos. Environ.*, **33**, 2337–2345, doi:10.1016/S1352-2310(98)00432-4.
- Frisch, U., 1996: *Turbulence: The Legacy of A. N. Kolmogorov*. Cambridge University Press, 312 pp.
- Garratt, J. R., 1994: *The Atmospheric Boundary Layer*. Cambridge University Press, 336 pp.
- Gioia, G., G. Lacorata, E. P. M. Filho, A. Mazzino, and U. Rizza, 2004: The Richardson's law in large-eddy simulations of

- boundary-layer flows. *Bound.-Layer Meteor.*, **113**, 187–199, doi:10.1023/B:BOUN.0000039373.45669.68.
- Gunatilaka, A., A. Skvortsov, and R. Gailis, 2012: High fidelity simulation of hazardous plume concentration time series based on models of turbulent dispersion. *Proc. 15th Int. Conf. on Information Fusion*, Singapore, ISIF, 2630–2637.
- He, X., G. He, and P. Tong, 2010: Small-scale turbulent fluctuations beyond Taylor's frozen-flow hypothesis. *Phys. Rev.*, **81**, 065303, doi:10.1103/PhysRevE.81.065303.
- Higgins, C. W., M. Froidevaux, V. Simeonov, N. Vercauteren, C. Barry, and M. Parlange, 2012: The effect of scale on the applicability of Taylor's frozen turbulence hypothesis in the atmospheric boundary layer. *Bound.-Layer Meteor.*, **143**, 379–391.
- Huang, J., X. Lee, and E. G. Patton, 2009: Dissimilarity of scalar transport in the convective boundary layer in inhomogeneous landscapes. *Bound.-Layer Meteor.*, **130**, 327–345, doi:10.1007/s10546-009-9356-8.
- Jamriska, M., T. C. DuBois, and A. Skvortsov, 2012: Statistical characterisation of bio-aerosol background in an urban environment. *Atmos. Environ.*, **54**, 439–448, doi:10.1016/j.atmosenv.2012.02.049.
- Klose, M., and Y. Shao, 2012: Stochastic parameterization of dust emission and application to convective atmospheric conditions. *Atmos. Chem. Phys. Discuss.*, **12**, 3263–3293, doi:10.5194/acpd-12-3263-2012.
- Kraichnan, R. H., 1968: Small-scale structure of a scalar field convected by turbulence. *Phys. Fluids*, **11**, 945–954, doi:10.1063/1.1692063.
- Kunnen, R., H. Clercx, B. J. Geurts, L. J. A. van Bokhoven, R. A. D. Akkermans, and R. Verzicco, 2008: Numerical and experimental investigation of structure-function scaling in turbulent Rayleigh-Bénard convection. *Phys. Rev.*, **77E**, 016302, doi:10.1103/PhysRevE.77.016302.
- Lanotte, A. S., and I. Mazzitelli, 2013: Scalar turbulence in convective boundary layers by changing the entrainment flux. *J. Atmos. Sci.*, **70**, 248–265.
- Lohse, D., and K.-Q. Xia, 2010: Small-scale properties of turbulent Rayleigh-Bénard convection. *Annu. Rev. Fluid Mech.*, **42**, 335–364, doi:10.1146/annurev.fluid.010908.165152.
- Luhar, A. K., M. F. Hibberd, and M. S. Borgas, 2000: A skewed meandering plume model for concentration statistics in the convective boundary layer. *Atmos. Environ.*, **34**, 3599–3616, doi:10.1016/S1352-2310(00)00111-4.
- Mazzitelli, I., and A. S. Lanotte, 2012: Active and passive scalar intermittent statistics in turbulent atmospheric convection. *Physica D*, **241**, 251–259, doi:10.1016/j.physd.2011.07.009.
- McNaughton, K. G., R. J. Clement, and J. B. Moncrieff, 2007: Scaling properties of velocity and temperature spectra above the surface friction layer in a convective atmospheric boundary layer. *Nonlinear Processes Geophys.*, **14**, 257–271, doi:10.5194/npg-14-257-2007.
- Mendis, C., A. Skvortsov, A. Gunatilaka, and S. Karunasekera, 2012: Performance of wireless chemical sensor network with dynamic collaboration. *IEEE Sens. J.*, **12**, 3–21, doi:10.1109/JSEN.2012.2198349.
- Mikkelsen, T., H. Jørgensen, M. Nielsen, and S. Ott, 2002: Similarity scaling of surface-released smoke plumes. *Bound.-Layer Meteor.*, **105**, 483–505, doi:10.1023/A:1020380820526.
- Monin, A. S., and A. M. Yaglom, 1975a: *Statistical Fluid Mechanics: Mechanics of Turbulence*. Vol. 1. MIT Press, 782 pp.
- , and —, 1975b: *Statistical Fluid Mechanics: Mechanics of Turbulence*. Vol. 2. MIT Press, 896 pp.
- Ottino, J. M., 1989: *The Kinematics of Mixing: Stretching, Chaos, and Transport*. Cambridge Texts in Applied Mathematics, Vol. 3, Cambridge University Press, 396 pp.
- Salazar, J., and L. Collins, 2009: Two-particle dispersion in isotropic turbulent flows. *Annu. Rev. Fluid Mech.*, **41**, 405–432, doi:10.1146/annurev.fluid.40.111406.102224.
- Schmitt, F., 2005: Explicit predictability and dispersion scaling exponents in fully developed turbulence. *Phys. Lett.*, **342A**, 448–458, doi:10.1016/j.physleta.2005.05.088.
- Shraiman, B., and E. Siggia, 2000: Scalar turbulence. *Nature*, **405**, 639–646, doi:10.1038/35015000.
- Siebesma, A. P., P. M. M. Soares, and J. Teixeira, 2007: A combined eddy-diffusivity mass-flux approach for the convective boundary layer. *J. Atmos. Sci.*, **64**, 1230–1248.
- Skvortsov, A., M. Jamriska, and T. C. DuBois, 2010: Scaling laws of passive tracer dispersion in the turbulent surface layer. *Phys. Rev.*, **82E**, 056304, doi:10.1103/PhysRevE.82.056304.
- Sofiev, M., V. Sofieva, T. Elperin, N. Kleeorin, I. Rogachevskii, and S. S. Zilitinkevich, 2009: Turbulent diffusion and turbulent thermal diffusion of aerosols in stratified atmospheric flows. *J. Geophys. Res.*, **114**, D18209, doi:10.1029/2009JD011765.
- Sreenivasan, K. R., and J. Schumacher, 2010: Lagrangian views on turbulent mixing of passive scalars. *Philos. Trans. Roy. Soc.*, **A368**, 1561–1577, doi:10.1098/rsta.2009.0140.
- Sullivan, P. P., C. H. Moeng, S. D. M. B. Stevens, and D. H. Lenschow, 1998: Structure of the entrainment zone capping the convective atmospheric boundary layer. *J. Atmos. Sci.*, **55**, 3042–3064.
- Sykes, R., 1988: Concentration fluctuations in dispersing plumes. *Lectures on Air Pollution Modeling*, A. Venkatram and J. C. Wyngaard, Eds., Amer. Meteor. Soc., 325–356.
- Toschi, F., and E. Bodenschatz, 2008: Lagrangian properties of particles in turbulence. *Annu. Rev. Fluid Mech.*, **41**, 375–404, doi:10.1146/annurev.fluid.010908.165210.
- Van Ulden, A. P., and A. A. M. Holtslag, 1985: Estimation of atmospheric boundary layer parameters for diffusion applications. *J. Climate Appl. Meteor.*, **24**, 1196–1207.
- Venkatram, A., 2004: The role of meteorological inputs in estimating dispersion from surface releases. *Atmos. Environ.*, **38**, 2439–2446, doi:10.1016/j.atmosenv.2004.02.005.
- Weil, J. C., R. I. Sykes, and A. Venkatram, 1992: Evaluating air-quality models: Review and outlook. *J. Appl. Meteor.*, **31**, 1121–1145.
- , P. P. Sullivan, E. G. Patton, and C.-H. Moeng, 2012: Statistical variability of dispersion in the convective boundary layer: Ensembles of simulations and observations. *Bound.-Layer Meteor.*, **145**, 185–210, doi:10.1007/s10546-012-9704-y.
- Wyngaard, J. C., 2010: *Turbulence in the Atmosphere*. Cambridge University Press, 406 pp.
- , and S. F. Clifford, 1977: Taylor's hypothesis and high-frequency turbulence spectra. *J. Atmos. Sci.*, **34**, 922–929.
- Yee, E., and R. Chan, 1997: Probability density function of concentration increments in a surface plume dispersing in the atmospheric boundary layer. *Phys. Lett.*, **227A**, 340–348, doi:10.1016/S0375-9601(97)00031-5.
- , and A. Skvortsov, 2011: Scalar fluctuations from a point source in a turbulent boundary layer. *Phys. Rev.*, **84E**, 036306, doi:10.1103/PhysRevE.84.036306.
- Zhou, Q., C.-M. Li, Z.-M. Lu, and Y.-L. Liu, 2011: Experimental investigation of longitudinal space-time correlations of the velocity field in turbulent Rayleigh-Bénard convection. *J. Fluid Mech.*, **683**, 94–111.

Copyright of Journal of the Atmospheric Sciences is the property of American Meteorological Society and its content may not be copied or emailed to multiple sites or posted to a listserv without the copyright holder's express written permission. However, users may print, download, or email articles for individual use.